REVIEWS

Rational design of multinary copper chalcogenide nanocrystals for photocatalytic hydrogen evolution

Hao Fu and Aiwei Tang†

Key Laboratory of Luminescence and Optical Information, Ministry of Education, School of Science, Beijing Jiaotong University, Beijing 100044, China

Abstract: Photocatalytic hydrogen evolution is one of the most promising ways to solve environmental problems and produce a sustainable energy source. To date, different types of photocatalysts have been developed and widely used in photocatalytic hydrogen evolution. Recently, multinary copper chalcogenides have attracted much attention and exhibited potential applications in photocatalytic hydrogen evolution due to their composition-tunable band gaps, diverse structures and environmental-benign characteristics. In this review, some progress on the synthesis and photocatalytic hydrogen evolution of multinary copper chalcogenide nanocrystals (NCs) was summarized. In particular, considerable attention was paid to the rational design and dimensional or structural regulation of multinary copper chalcogenide NCs. Importantly, the photocatalytic hydrogen evolution of multinary copper chalcogenide NCs were reviewed from the aspects of energy level structures, crystal facets, morphology as well as composition. Finally, the current challenges and future perspectives of copper chalcogenide were proposed.

Key words: photocatalytic hydrogen evolution; nanocrystals; copper chalcogenides

1. Introduction

Thanks to the demands of ever-increasing productivity in the global economy, the demand for energy is growing daily[1–3]. Fossil fuels have been our major energy source for hundreds of years, and more than 80% part of the current energy supply still focuses on carbon-based energy sources, which leads to a lot of environmental problems, such as climate change, greenhouse effect, and air pollution[4, 5]. Thus, the development of sustainable green energy sources has become an urgent scientific challenge. In the past decades, great efforts have been made to exploit alternative energy sources. Among all the solutions, hydrogen is considered to be the most promising one due to its high energy capacity and environmentally friendly characteristics[6–8]. For a typical photocatalytic process, the first step is the light absorption of the semiconductor photocatalysts — the photo-excited charges (electrons and holes) are generated during this process. Then, the excited charges are separated, migrated, or transferred individually. Finally, the excited charges are transferred to the surface of the material and participated in the decomposition of water to produce hydrogen. As a matter of fact, all of these processes affect the final generation of hydrogen from the semiconductor photocatalysts. After decades of effort, photocatalytic hydrogen production technology has now begun to bear fruit. To date, several different types of materials have been developed to produce hydrogen energy, in which the semiconductors have become one of the most popular materials for photocatalytic hydrogen evolution[9–13]. For

example, TiO$_2$ is the first reported photocatalyst for water splitting under UV light, which exhibits high efficiency and stability[14–16]. Moreover, compounds such as cadmium-based semiconductors have also been developed as novel photocatalysts because they have suitable band gaps for sunlight absorption[17–19]. However, among these photocatalysts, TiO$_2$ mainly absorbs ultraviolet light and it cannot maximize the solar energy. As for the cadmium-based semiconductors, the intrinsic toxicity limits their further application because of the presence of the heavy elements in the compounds[20]. Therefore, the development of new alternative semiconductor materials for photocatalytic applications is in great demand.

In recent years, multinary copper chalcogenide semiconductor NCs have attracted considerable and growing attention due to their abundance, low cost, reduced environmental and health impact and appropriate direct band gaps for sunlight absorption[21, 22]. More importantly, their structure, composition, and stoichiometry can be easily regulated, which leads to a huge material family from binary to quaternary involving a large number of elements[23–25]. Their excellent characteristics give them a wide range of applications in many different fields, such as LEDs, solar cells, photodetectors and photocatalysis[26–30]. Research towards multinary copper chalcogenides starts from their binary counterparts, such as Cu$_{2-x}$S. These binary compounds have been widely studied because of their tunable localized surface plasmon resonance (LSPR) absorption in near-infrared region[31–35]. In addition, the presence of Cu vacancies in the binary compounds offers an opportunity to rationally design and synthesize multinary Cu chalcogenides NCs through a cation exchange strategy[36].

Since the wider response range of solar light, tunable bandgap, as well as the environmental-benign characteristics, the cadmium-free multinary Cu chalcogenides compounds
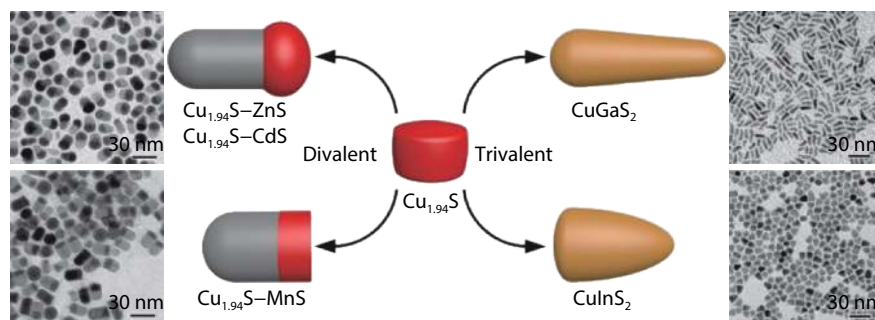
Fig. 1. (Color online) Schematic illustration and TEM images of the product evolution from $Cu_{1.94}S$ NCs to different types of heterostructured and alloyed NCs[53].

have drawn great interest for photocatalytic hydrogen production. Although the earlier work on the photocatalytic H_2 evolution of $CuInS_2$ was reported in 1992, the efficiency was much lower than that of other photocatalysts[37]. After tens of years development, much progress has been made in the improvement of the photocatalytic performance of the copper chalcogenide compounds[38–41]. For example, Tan *et al.* introduced Zn into $CuInS_2$ compounds and studied the effects of different copper contents on the photocatalytic performance of Cu–In–Zn–S NCs[42]. Similarly, Kandie *et al.* introduced Zn into Cu–Ga–S NCs and compared the photocatalytic properties of the samples with different Zn contents[43]. Besides, Yu *et al.* synthesized $CuIn_xGa_{1-x}S_2$ nanorods with nonstoichiometric ratio by adding Ga elements into $CuInS_2$ nanorods[44]. It was found that the photocatalytic performance of the products was improved by introducing Ga into the ternary $CuInS_2$ NCs. Moreover, Zhao *et al.* constructing $CuGaS_2$–ZnS p–n type nanoheterostructures based on $CuGaS_2$ and ZnS compounds through a solution route, and the photocatalytic performance of the heterostructured NCs was significantly increased[45]. To date, the photocatalytic hydrogen evolution of multinary copper chalcogenide NCs has become a popular research topic. Very recently, our group focused on the rational design and synthesis of ternary and quaternary copper chalcogenide NCs and their applications in the photocatalytic hydrogen evolution. In this review, we first introduce the rational design and synthesis of copper chalcogenides NCs with different morphology and composition through a colloidal chemical method. We also summarize the effects of the key parameters including morphology, crystal facets and energy level structure on the photocatalytic hydrogen evolution of the NCs. Finally, the perspectives and future challenges for the next research in the copper chalcogenide photocatalysts are proposed.

2. Rational design and synthesis of copper chalcogenide NCs

Given the high cation mobility of Cu^+ ions at a relatively high temperature, the ternary and quaternary copper chalcogenides are actually derived from the binary ones through substituting or replacing some of the cations, while they still retain their original structures[46–48]. During the synthesis of copper chalcogenide NCs through a colloidal synthesis method, the combination of ions and the formation of crystals generally follow the Hard–Soft–Acid–Base (HSAB) Theory[49, 50] and the LaMer Classical Nucleation Theory[51, 52]. Thanks to these

points, it is easier to realize the controllable synthesis of copper chalcogenide NCs with different morphologies and compositions as well as the energy level structures.

2.1. Synthesis of heterostructured and alloyed NCs from binary $Cu_{1.94}S$ NCs

The cation exchange method has often been used to prepare different types of copper chalcogenide NCs since the copper ions in nonstoichiometric $Cu_{2-x}S$ NCs had a very high mobility at high temperature, which acted as the seeds for the formation of heterostructured and alloyed NCs. Our recent work showed the synthesis of heterostructured and alloyed NCs by introducing different valent metal ions, such as Zn^{2+}, Cd^{2+}, Mn^{2+}, In^{3+} and Ga^{3+}, into the monoclinic $Cu_{1.94}S$ NCs[53]. Theoretically, they should all form ternary alloyed NCs, but, interestingly, it was only formed by adding trivalent cation precursors. However, it is the heterogeneous structures that formed in the addition of divalent cation precursors. A schematic illustration of the products evolution from binary NCs to the heterostructured and alloyed NCs is shown in Fig. 1, and the corresponding transmission electron microscopy (TEM) images are also given. All the heterostructured and alloyed NCs are synthesized by introducing different metal compounds precursors into the mixture of copper precursors and 1-dodecanethiol at a relatively high temperature under N_2 protection.

Very interestingly, the ternary alloyed NCs, such as $CuInS_2$ and $CuGaS_2$, also underwent heterostructured intermediates during their formation. In the process, cation exchange was taken place to incorporate trivalent ions into the $Cu_{1.94}S$ seeds, followed by the formation of $Cu_{1.94}S$–$CuInS_2$ or $Cu_{1.94}S$–$CuGaS_2$ heterostructured NCs. Further prolonging the reaction time resulted in the cation inter-diffusion across the whole nanocrystals, gradually leading to the formation of $CuInS_2$ and $CuGaS_2$ alloyed NCs[23, 54, 55]. As to the heterostructured $Cu_{1.94}S$–ZnS or $Cu_{1.94}S$–CdS NCs, a typical cation exchange process would take place firstly, in which the divalent cations entered the $Cu_{1.94}S$ seeds. With the enrichment of the secondary cations, they could bond with S^{2-} and nucleate on the preformed domains, leading to the epitaxial growth along the anionic framework. As a result, they turned out to be heterogeneous structures[56, 57]. According to Zhao's work, such epitaxial growth may have resulted from the small difference between the surface tension of the two parts[58, 59]. Moreover, previous reports pointed out that the Cu content was very low in the ZnS:Cu system without any chemical co-activator like Ga[60], which may be responsible for the forma-
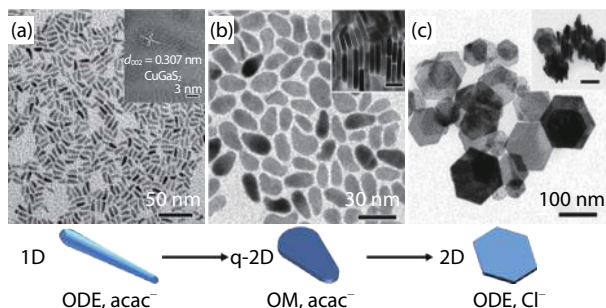
Fig. 2. TEM images and morphology diagrams of 1D, quasi-2D and 2D CuGaS$_2$ NCs[64].

tion of heterostructured compound but not alloyed one by adding Zn^{2+} to the Cu$_{1.94}$S alone.

2.2. Dimensional regulation of ternary CuGaS$_2$ NCs

Since the ternary alloyed NCs could be synthesized by introducing trivalent ions into the Cu$_{1.94}$S seeds through a cation exchange method, the morphology was tuned in a limited scope[61–63]. Our recent work reported the dimensional regulation of the CuGaS$_2$ NCs, which offered an effective approach for tuning the dimension and thus boosted the photocatalytic performance[64]. In this work, ternary CuGaS$_2$ NCs were synthesized by using a one-step heating-up process without any injection, which had a hexagonal wurtzite structure. The dimension of the NCs varied from one-dimensional (1D) to two-dimensional (2D) by tuning the surfactants, and the TEM images are depicted in Fig. 2. The 1D nanorods were synthesized with Cu(acac)$_2$ and Ga(acac)$_3$ as precursors, 1-octadecene (ODE) as solvents and dodecane thiol (DDT) as sulfur sources. These can be regarded as the original conditions and the morphology of the as-obtained samples were essentially identical to that of the previous work[53]. The qusi-2D tennis-racket-shaped NCs were synthesized through the original method but to replace some of the solvent with oleylamine (OM). While the synthetic conditions of 2D hexagonal nanosheets were basically the same as original method except that Ga(acac)$_3$ was replaced by GaCl$_3$, and the presence of Cl$^-$ plays a significant role in the formation of 2D nanosheets.

Further study indicated that the different dimensional NCs were from the difference in the growth direction, which is caused by the adsorption of added ligands to a certain crystal facet. Specifically, the amine molecules preferred to coordinate with cations on the (001) facet of wurtzite NCs[65], and the Cl$^-$ specifically adsorbed on the {001} and {110} facets. The growth in the direction of the adsorbed crystal facets could be inhibited, so they finally formed the tennis-racket-shaped NCs and hexagonal nanosheets, respectively.

2.3. Synthesis of L-shaped quaternary Cu–Ga–Zn–S NCs

In the previous narratives, adding Ga^{3+} and Zn^{2+} into binary Cu$_{1.94}$S NCs could lead to the formation of ternary alloyed and heterostructured NCs, respectively. Surprisingly, our previous work showed that quaternary Cu–Ga–Zn–S nanocrystals with special L-shaped (Figs. 3(a) and 3(b)) were synthesized by simultaneously introducing Ga(acac)$_3$ and Zn(acac)$_2$ into the binary NCs[66].

By further studying the temporal evolution of the morpho-

logy and crystal structure of the products, it was confirmed that the formation of quaternary and L-shaped Cu–Ga–Zn–S NCs was related to the transformation from the binary Cu$_{1.94}$S to Cu$_{31}$S$_{16}$–ZnS and Cu$_{31}$S$_{16}$–CuGaZnS nanoheterogeneous structures caused by the inter-diffusion of Zn^{2+} and Ga^{3+} into the Cu$_{1.94}$S seeds. In particular, on the one hand, the formation of quaternary Cu–Ga–Zn–S NCs was by the synergistic effects of both Ga^{3+} and Zn^{2+} ions. On the other hand, the formation of L-shaped novel morphology was the result of careful regulation of reaction temperature, the concentrations of DDT and other factors[66].

3. Photocatalytic performance of copper chalcogenide NCs

The photocatalytic hydrogen evolution is essentially a process in which the electrons of the valence band are excited to the conduction band by optical excitation to participate in a chemical reaction[67]. As a result, the performance of a photocatalyst mainly depends on its energy band structure, which determines the ability of light absorption to ensure that the subsequent reaction would proceed smoothly. As the size is decreased to nanometer level, the crystal size has shrunk so dramatically that the surface energy could not be ignored[68]. Thus, the energy difference between the different crystal facets is greatly amplified and the exposed crystal facets are of particular importance[69, 70]. Fortunately, it is feasible to change the exposed crystal facets by adjusting the dimension of NCs. In addition, especially for the copper chalcogenides NCs, the element constituents also have a huge impact on their photocatalytic performance[42, 43].

In the aforementioned section, the synthetic issues from three studies were introduced, and formation mechanism of the different types of NCs was provided. However, for the photocatalytic applications, the parameters change of the NCs involved in these studies actually have deeper implications, which manifest themselves as changes in the energy-level structure, the crystal surface, and the elements of the NCs. Therefore, in the following sections, several important factors, which affect the photocatalytic hydrogen production of copper chalcogenide NCs, will be summarized and discussed from the aspects of energy level structure, crystal facets and composition, respectively.

3.1. Effects of energy level structure

In Zhu's work, two types of copper chalcogenide NCs were prepared by introducing different valent cations into the parent NCs. The photocatalytic hydrogen evolution of the alloyed and heterostructured NCs was compared, and the results are shown in Fig. 4[53]. It is found that the photocatalytic performance of both heterostructured and alloyed NCs were better than that of binary Cu$_{1.94}$S NCs, except for CuInS$_2$ NCs. Among them, Cu$_{1.94}$S–CdS and CuGaS$_2$ had the best performance. The main reason for these differences is that they have different energy level structures. From the energy level diagram (Fig. 4(c)), it can be derived that only Cu$_{1.94}$S–CdS NCs belong to the type II heterostructure out of the three samples, whose energy level structure is well suited to photocatalysis[71]. As for the alloyed NCs, it is now widely accepted that incorporation of the In and Ga ions into Cu$_{1.94}$S NCs could reduce the number of Cu vacancies, which is favored for the photocatalysis[53]. However, the conduction band min-
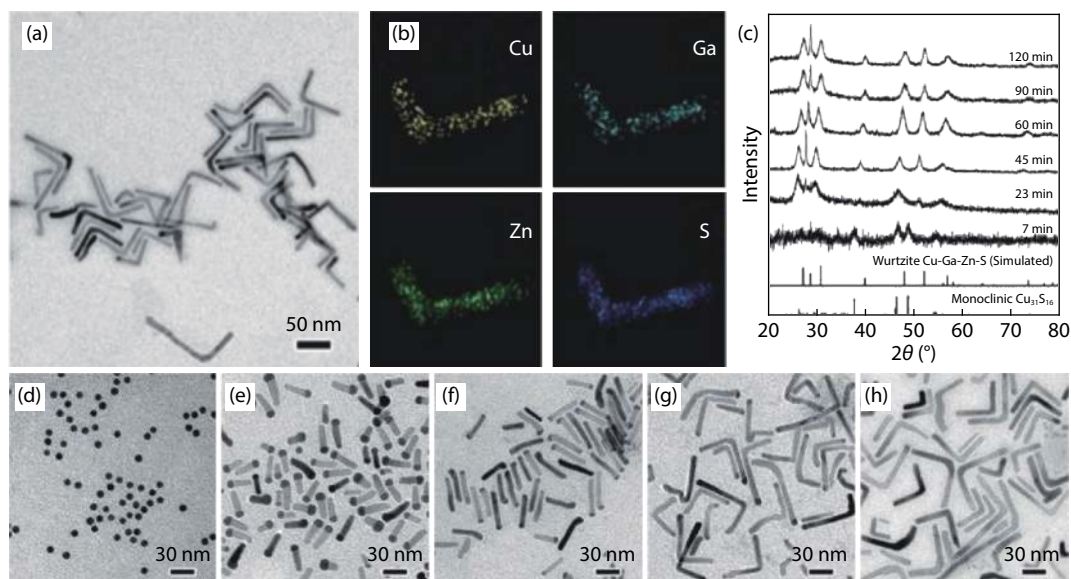
Fig. 3. (a) TEM images and (b) STEM-EDS elemental mapping images of the L-shaped Cu–Ga–Zn–S NCs. (c) XRD patterns of the products obtained at different reaction time. (d–h) TEM images of wurtzite Cu–Ga–Zn–S NCs synthesized at 240 °C for different reaction time: (d) 7 min, (e) 23 min, (f) 45 min, (g) 60 min, and (h) 120 min[66].
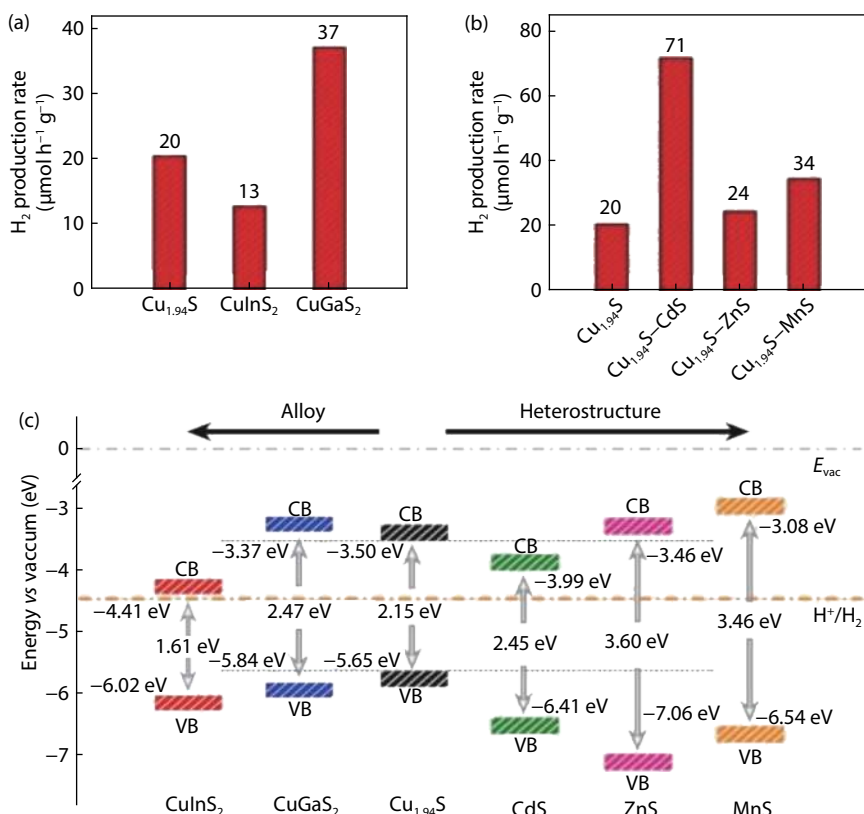

Fig. 4. (Color online) (a) The hydrogen production rate of the $Cu_{1.94}S$ NCs, $CuInS_2$ and $CuGaS_2$ alloyed NCs. (b) The hydrogen production rate of $Cu_{1.94}S$ NCs, $Cu_{1.94}S–ZnS$, $Cu_{1.94}S–CdS$ and $Cu_{1.94}S–MnS$ heterostructured NCs. (c) The energy level diagram of $Cu_{1.94}S$ NCs (black), $CuInS_2$ alloyed NCs (red), $CuGaS_2$ alloyed NCs (blue), $Cu_{1.94}S–ZnS$ (pink), $Cu_{1.94}S–CdS$ (green) and $Cu_{1.94}S–MnS$ heterostructured NCs (orange)[53].

imum (CBM) position of $CuInS_2$ is too low relative to H^+/H_2 to reduce H^+ back to hydrogen. This is the reason why the $CuInS_2$ alloyed NCs showed a decreased photocatalytic ability of hydrogen evolution. While the $CuGaS_2$ alloyed NCs had a suitable band gap that was preferred for the charge transport and separation, leading to an increase of photocatalytic performance[20, 72].

3.2. Effects of crystal facets

The energy level structures of different crystals could vary considerably, but actually, there are great differences between the facets' energies of the same crystal[69, 70]. According to the results mentioned above, all the three $CuGaS_2$ NCs with different dimensions have the wurtzite structure but the
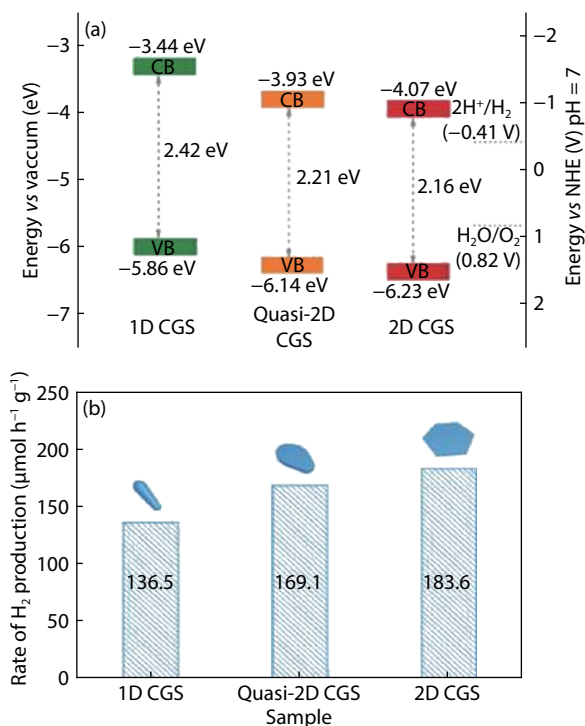
Fig. 5. (Color online) (a) The energy level diagrams of 1D, quasi-2D and 2D CuGaS$_2$ NCs. (b) The photocatalytic hydrogen production rates of 1D, quasi-2D and 2D CuGaS$_2$ NCs.

energy level of the three sample[64] is different. From the energy level structure diagram (Fig. 5(a)), it can be seen that the CBM position of 1D CuGaS$_2$ nanorods is the highest among the three samples, while that of the 2D samples is the lowest of all. Based on the previous report, the CBM of 2D CuGaS$_2$ NCs is lower than that of the other two counterparts, and its photocatalytic performance may be reduced. However, the 2D samples have the best photocatalytic performance[64].

The difference in morphology between 1D and 2D CuGaS$_2$ NCs is actually the difference in the exposed crystal facets. 2D CuGaS$_2$ NCs mainly expose more {001} facets and the 1D CuGaS$_2$ NCs prefer to expose {100} facets. The density functional theory (DFT) calculations were performed to study the properties of (001) and (100) surfaces, as shown in Fig. 6. On the one hand, it can be derived from the work function of the CuGaS$_2$ (001) and (100) that it was easier for the electrons escaping from the (001) surface than the (100) surface (Figs. 6(c) and 6(d)). That is to say, it is easier for the (001) surface to generate photoelectrons. On the other hand, the projected density of states (PDOS) of the (001) and (100) surfaces (Figs. 6(e) and 6(f)) represented that the (001) surface had some metal properties, while the (100) surface did not, which indicated that the (001) surface had much better property of charge transport[73]. For these reasons, although 1D and 2D CuGaS$_2$ NCs have the same crystal structure, they are exposed to different crystal surfaces, resulting in a large difference in the photocatalytic performance.

In this work, the different dimensions of CuGaS$_2$ NCs originate from the specific binding of ligands to the crystal facets, and interestingly, the exposed facets then lead to the different photocatalytic properties. Subsequent research can be inspired by the deliberate exposure of a certain surface with high energy.

3.3. Synergistic effects of composition and morphology

The L-shaped Cu–Ga–Zn–S alloyed NCs is a great success in the synthesis of copper chalcogenide NCs. Besides, such samples also show an excellent performance in photocatalytic hydrogen evolution compared with the binary and ternary counterparts (as shown in Fig. 7)[66]. The reason for the great improvement in the photocatalytic performance of the L-shaped CGZS NCs can be explained in two aspects: composition and morphology. Firstly, adding Zn^{2+} ions into the p-type semiconductor CuGaS$_2$ NCs would greatly reduce the number of original Cu vacancies, which could capture part of the photogenerated electrons. Thus, the separation efficiency of photon-generated carriers could be greatly improved, and the photocatalytic performance of the NCs could also be improved[43, 45]. Besides, the novel morphology also played an important role in improving the photocatalytic performance. The L-shaped CGZS nanorods represented a one-dimensional form and had enough length, which offered the carriers a direct transporting path[74]. In this way, the carrier separation ability of the L-shaped CGZS NCs was further improved.

4. Photostability of multinary copper chalcogenide NCs

Photostability is an important parameter to evaluate the photocatalytic performance of a semiconductor photocatalyst, which is the prerequisite for further practical application. Only a little loss is observed in the Cu$_{1.94}$S–CdS heterostructured NCs and only Cu$_{1.94}$S NCs over 20 h after 5 consecutive runs under solar illumination with the intensity of 100 mW/cm^2, demonstrating their good photocatalytic stability for hydrogen production (Fig. 8(a)). Moreover, for the L-shaped CGZS nanorods, there is no obvious reduction in the hydrogen production rate after six cycles under solar light with the intensity of 300 mW/cm^2, which indicates that the product shows a good photostability (Fig. 8(a)). Therefore, all the copper chalcogenide NCs, including alloyed and heterostructured as well as ternary or quaternary NCs, have relatively good photostability, which may hold a promising potential in the further applications.

5. Conclusions and perspectives

In summary, we introduced some representative works on the synthesis and photocatalytic hydrogen evolution of multinary copper chalcogenide NCs, and the photocatalytic performance could be improved by tailoring the energy level structure, crystal facets and composition, which could be tailored by tuning the synthetic parameters. For example, the incorporation of divalent and trivalent metal cations into binary Cu$_{1.94}$S seeds could bear heterostructured and alloyed NCs, which exhibited different energy level structures, leading to different photocatalytic performance. In contrast, quaternary Cu–Ga–Zn–S alloyed NCs could be formed by introducing Ga^{3+} and Zn^{2+} ions at the same time, and the incorporation of Zn would reduce the Cu vacancies and the spatial effect of L-shaped morphology would offer a positive effect on the separation and migration of carriers, which contributed to the improved photocatalytic hydrogen evolution.

Despite remarkable achievements obtained in the photocatalytic performance of the copper chalcogenide NCs,
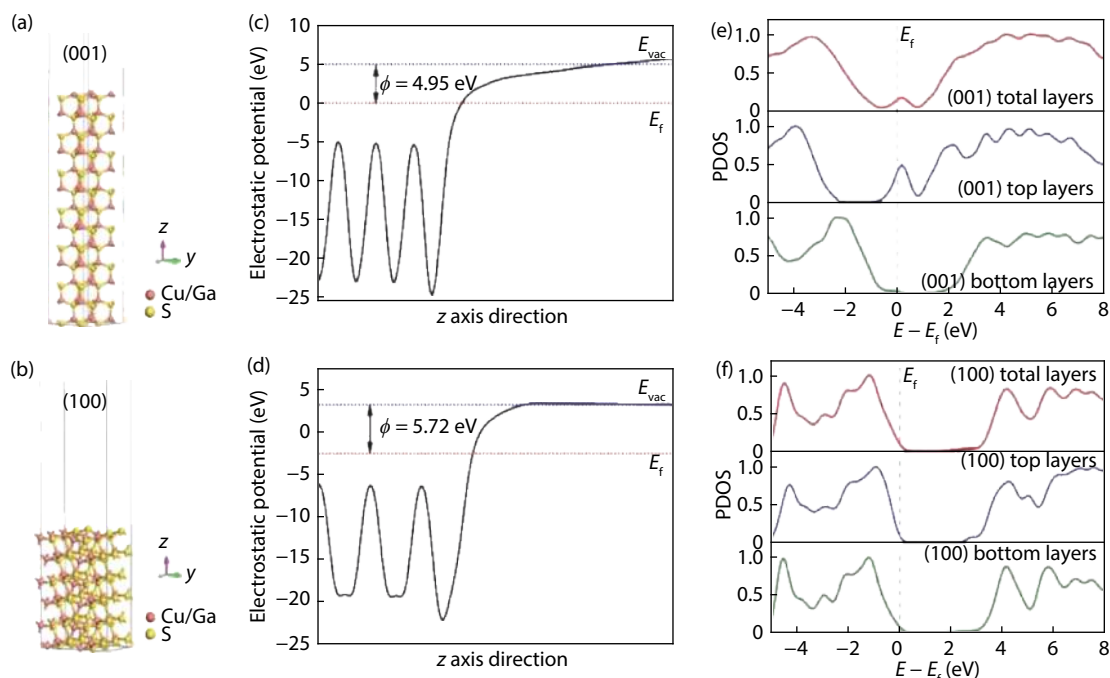
Fig. 6. (Color online) Schematic models of the (a) (001) surface and (b) (100) surface of stimulated wurtzite CuGaS$_2$ after geometry optimization. Work function for the (c) CuGaS$_2$ (001) surface and (d) (100) surface. The calculated PDOS for (e) CuGaS$_2$ (001) and (f) (100) surfaces, where the PDOS contains the total layer surface, top layer surface and bottom layer surface for simulated every surface[64].
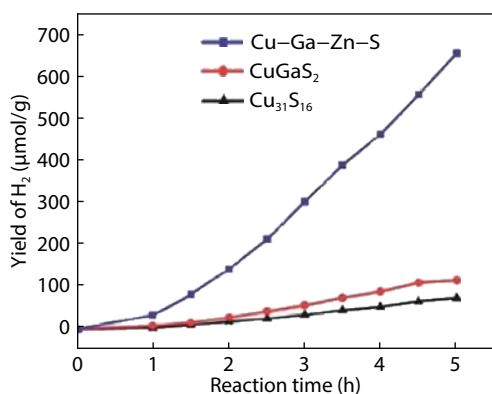

Fig. 7. Photocatalytic hydrogen evolution of binary Cu$_{31}$S$_{16}$ NCs, ternary CuGaS$_2$ NCs and quaternary L-shaped Cu–Ga–Zn–S nanorods[66].

Fig. 8. (Color online) Cycling tests of hydrogen production for (a) Cu$_{1.94}$S–CdS (red) and Cu$_{1.94}$S (black) NCs and (b) L-shaped Cu–Ga–Zn–S nanorods under simulated solar illumination[66].

there still exist many issues to be addressed and plenty of challenges to be defeated in the future work. For example, more in-depth studies are needed to study the mechanism of the action of Zn^{2+} and its optimal concentration in the Cu–Ga–Zn–S alloyed NCs. The low photocatalytic efficiency and the lack of extensive studies for a successful scale-up of the laboratory setup into an industrially relevant scale. The effects of different metal elements for multinary copper chalcogenide NCs on photocatalytic hydrogen production are still debating. Overall, there is much room to boost the photocatalytic efficiency of copper chalcogenide NCs as compared to other photocatalysts.

Acknowledgements

References

[1]   Chow J. Energy resources and global development. Science, 2003, 302(5650), 1528

[2]   Dincer I, Rosen M A. Energy, environment and sustainable development. Appl Energy, 1999, 64(1), 427

[3]   Hoffmann M R, Martin S T, Choi W, et al. Environmental applications of semiconductor photocatalysis. Chem Rev, 1995, 95(1), 69

[4]   Armaroli N, Balzani V. The future of energy supply: Challenges

and opportunities. Angew Chem Int Ed, 2007, 46, 52

[5] L i, X, Yu J G, Low J X, et al. Engineering heterogeneous semiconductors for solar water splitting. J Mater Chem A, 2015, 3, 2485

[6] Cook T R, Dogutan D K, Reece S Y, et al. Solar energy supply and storage for the legacy and nonlegacy worlds. Chem Rev, 2010, 11, 6474

[7] Muradov N Z, Veziroglu T N. "Green" path from fossil-based to hydrogen economy: An overview of carbon-neutral technologies. Int J Hydrogen Energy, 2008, 33(23), 6804

[8] Takanabe K, Domen K. Toward visible light response: Overall water splitting using heterogeneous photocatalysts. Green, 2011, 1(4), 313

[9] Xu C Q, Anusuyadevi P R, Aymonier C, et al. Nanostructured materials for photocatalysis. Chem Soc Rev, 2019, 48, 3868

[10] Kudo A, Miseki Y. Heterogeneous photocatalyst materials for water splitting. Chem Soc Rev, 2009, 38, 253

[11] Shinde S S, Bhosale C H, Rajpure K Y. Solar light assisted photocatalysis of water using a zinc oxide semiconductor. J Semicond, 2013, 34(4), 043002

[12] Huang Y B, Liu J, Deng Y C, et al. The application of perovskite materials in solar water splitting. J Semicond, 2020, 41(1), 011701

[13] Xiang Q, Yu J, Jaroniec M. Graphene-based semiconductor photocatalysts. Chem Soc Rev, 2012, 41(2), 782

[14] Schneider J, Matsuoka M, Takeuchi M, et al. Understanding TiO_2 photocatalysis: mechanisms and materials. Chem Rev, 2014, 114(19), 9919

[15] Peng L, Liu Y, Li Y, et al. Fluorine-assisted structural engineering of colloidal anatase TiO_2 hierarchical nanocrystals for enhanced photocatalytic hydrogen production. Nanoscale, 2019, 11, 22575

[16] Xu H, Reunchan P, Ouyang S, et al. Anatase TiO_2 single crystals exposed with high-reactive {111} facets toward efficient H_2 evolution. Chem Mater, 2013, 25(3), 405

[17] Preethi V, Kanmani S. Photocatalytic hydrogen production. Mater Sci Semicond Process, 2013, 16, 561

[18] Jang J S, Kim H G, Borse P H. Simultaneous hydrogen production and decomposition of dissolved in alkaline water over composite photocatalysts under visible light irradiation. Int J Hydrogen Energy, 2007, 32, 4786

[19] Costi R, Saunders A E, Elmalem E, et al. Visible light-induced charge retention and photocatalysis with hybrid CdSe–Au nanodumbbells. Nano Lett, 2008, 8(2), 637

[20] Chen X B, Shen S H, Guo L J, et al. Semiconductor-based photocatalytic hydrogen generation. Chem Rev, 2010, 110(11), 6503

[21] Coughlan C, Ibánez M, Dobrozhan O, et al. Compound copper chalcogenide nanocrystals. Chem Rev, 2017, 117(9), 5865

[22] Sun S D, Li P J, Liang S H, et al. Diversified copper sulfide ($Cu_{2-x}S$) micro-/nanostructures: a comprehensive review on synthesis, modifications and applications. Nanoscale, 2017, 9(32), 11357

[23] Tang A W, Hu Z L, Yin Z, et al. One-pot synthesis of $CuInS_2$ nanocrystals using different anions to engineer their morphology and crystal phase. Dalton Trans, 2015, 44(19), 9251

[24] Trizio D L, Manna L. Forging colloidal nanostructures via cation exchange reactions. Chem Rev, 2016, 116, 10852

[25] Chen B K, Chang S, Li D Y, et al. Template synthesis of $CuInS_2$ nanocrystals from In_2S_3 nanoplates and their application as counter electrodes in dye-sensitized solar cells. Chem Mater, 2015, 27, 5949

[26] Hages C J, Levcenco S, Miskin C K, et al. Improved performance of Ge-alloyed CZTGeSSe thin-film solar cells through control of elemental losses. Prog Photovolt Res Appl, 2013, 23(3), 376

[27] Wang L J, Guan Z Y, Tang A W. Multinary copper-based chalcogenide semiconductor nanocrystals: synthesis and applications in light-emitting diodes and bioimaging. J Nanopart Res, 2020, 22(1), 1

[28] Guan Z Y, Tang A W, Lv P W, et al. new insights into the formation and color-tunable optical properties of multinary Cu–In–Zn-based chalcogenide semiconductor nanocrystals. Adv Opt Mater, 2018, 6, 1701389

[29] Guan Z Y, Chen F, Liu Z Y, et al. Compositional engineering of multinary Cu–In–Zn-based semiconductor nanocrystals for efficient and solution-processed red-emitting quantum-dot light-emitting diodes. Organ Electron, 2019, 74, 46

[30] Kim B Y, Kim J H, Lee K H, et al. Synthesis of highly efficient azure-to-blue-emitting Zn–Cu–Ga–S quantum dots. Chem Commun, 2017, 53(29), 4088

[31] Li X, Tang A W, et al. Effects of alkanethiols chain length on the synthesis of $Cu_{2-x}S$ nanocrystals: phase, morphology, plasmonic properties and electrical conductivity. RSC Adv, 2014, 4, 54547

[32] Ye H H, Tang A W, Yang C H, et al. Synthesis of $Cu_{2-x}S$ nanocrystals induced by foreign metal ions: phase and morphology transformation and localized surface plasmon resonance. CrystEngComm, 2014, 16(37), 8684

[33] Zhu D X, Tang A W, Ye H H, et al. Tunable near-infrared localized surface plasmon resonances of djurleite nanocrystals: effects of size, shape, surface-ligands and oxygen exposure time. J Mater Chem C, 2015, 3(26), 6686

[34] Zhu D X, Tang A W, Peng L, et al. Tuning the plasmonic resonance of $Cu_{2-x}S$ nanocrystals: effects of the crystal phase, morphology and surface ligands. J Mater Chem C, 2016, 4(22), 4880

[35] Chen M M, Xue H G, Guo S P. Multinary metal chalcogenides with tetrahedral structures for second-order nonlinear optical, photocatalytic, and photovoltaic applications. Coordin Chem Rev, 2018, 368, 115

[36] Nethravathi C, Ragesh R N, Rajamathi J T, et al. Microwave-assisted synthesis of porous aggregates of CuS nanoparticles for sunlight photocatalysis. ACS Omega, 2019, 4(3), 4825

[37] Kobayakawa K, Teranishi A, Tsurumaki T, et al. Photocatalytic activity of $CuInS_2$ and $CuIn_5S_8$. Electrochim Acta, 1992, 37(3), 465

[38] Kaga H, Tsutsui Y, Nagane A, et al. An effect of Ag(I)-substitution at Cu sites in $CuGaS_2$ on photocatalytic and photoelectrochemical properties for solar hydrogen evolution. J Mater Chem A, 2015, 3(43), 21815

[39] Fan X B, Yu S, Zhan F, et al. Nonstoichiometric Cu_xIn_yS quantum dots for efficient photocatalytic hydrogen evolution. ChemSusChem, 2017, 10(24), 4833

[40] Yi L X, Liu Y Y, Yang N L, et al. One dimensional $CuInS_2$–ZnS heterostructured nanomaterials as low-cost and high-performance counter electrodes of dye-sensitized solar cells. Energy Environ Sci, 2013, 6(3), 835

[41] Yu Z J, Chen Z, Chen Y G, et al. Photocatalytic hydrogenation of nitroarenes using $Cu_{1.94}S$–$Zn_{0.23}Cd_{0.77}S$ heteronanorods. Nano Res, 2018, 11(7), 3730

[42] Tan L L, Liu Y H, Mao B D, et al. Effective bandgap narrowing of Cu–In–Zn–S quantum dots for photocatalytic H_2 production via cocatalyst-alleviated charge recombination. Inorgan Chem Front, 2018, 5(1), 258

[43] Kandiel T A, Anjum D H, Sautet P, et al. Electronic structure and photocatalytic activity of wurtzite Cu–Ga–S nanocrystals and their Zn substitution. J Mater Chem A, 2015, 3(16), 8896

[44] Yu X L, An X Q, Shavel A, et al. The effect of the Ga content on the photocatalytic hydrogen evolution of $CuIn_{1-x}Ga_xS_2$ nanocrystals. J Mater Chem A, 2014, 2(31), 12317

[45] Zhao M S, Huang F, Lin H, et al. $CuGaS_2$–ZnS p–n nanoheterostructures: a promising visible light photo-catalyst for water-splitting hydrogen production. Nanoscale, 2016, 8(37), 16670

[46] Kuzuya T, Hamanaka Y, Itoh K, et al. Phase control and its mechanism of $CuInS_2$ nanoparticles. J Colloid Interface Sci, 2012, 388(1), 137

[47] Khan M D, Akhtar J, Malik M A, et al. Tuning the phase and shape of copper sulfide nanostructures using mixed solvent systems. Chem Select, 2016, 1(18), 5982

[48] Fan F J, Wu L, Yu S H. Energetic I–III–VI$_2$ and I$_2$–II–IV–VI$_4$ nanocrys-

tals: synthesis, photovoltaic and thermoelectric applications. Energy Environ Sci, 2014, 7(1), 190

[49] Pearson G. Hard and soft acids and bases. Survey Progress Chem, 1969, 5(22), 1

[50] Nag A, Kovalenko M V, Lee J S, et al. Metal-free inorganic ligands for colloidal nanocrystals: S^{2-}, HS^-, Se^{2-}, HSe^-, Te^{2-}, HTe^-, TeS_3^{2-}, OH^-, and NH^{2-} as surface ligands. J Am Chem Soc, 2011, 133(27), 10612

[51] Lamer V K, Dinegar R H. Theory, production and mechanism of formation of monodispersed hydrosols. J Am Chem Soc, 1950, 11(72), 4847

[52] Xia Y N, Xiong Y J, Lim B, et al. Shape-controlled synthesis of metal nanocrystals: Simple chemistry meets complex physics. Angew Chem Int Ed, 2009, 48(1), 335

[53] Zhu D X, Ye H H, Liu Z M, et al. Seed-mediated growth of heterostructured $Cu_{1.94}$S-MS (M = Zn, Cd, Mn) and alloyed $CuNS_2$ (N = In, Ga) nanocrystals with structure- and composition-dependent photocatalytic hydrogen evolution. Nanoscale, 2020, 12(10), 6111

[54] Coppel Y, Spataro G, Pagès C, et al. Full characterization of colloidal solutions of long-alkyl-chain-amine-stabilized ZnO nanoparticles by NMR spectroscopy: Surface state, equilibria, and affinity. Chem Eur J, 2012, 18(17), 5384

[55] Kruszynska M, Borchert H, Parisi J, et al. Synthesis and shape control of $CuInS_2$ nanoparticles. J Am Chem Soc, 2010, 132(45), 15976

[56] Connor S T, Hsu C M, Weil B D, et al. Phase transformation of biphasic Cu_2S–$CuInS_2$ to monophasic $CuInS_2$ Nanorods. J Am Chem Soc, 2009, 131(13), 4962

[57] Yi L X, Gao M Y. From ultrathin two-dimensional djurleite nanosheets to one-dimensional nanorods comprised of djurleite nanoplates: Synthesis, characterization, and formation mechanism. Cryst Growth Des, 2011, 11(4), 1109

[58] Yang T Y, Wei L J, Jing L Y, et al. Dumbbell-shaped bi-component mesoporous janus solid nanoparticles for biphasic interface catalysis. Angew Chem Int Ed, 2017, 56(29), 8459

[59] Li X M, Zhou L, Wei Y, et al. Anisotropic growth-induced synthesis of dual-compartment janus mesoporous silica nanoparticles for bimodal triggered drugs delivery. J Am Chem Soc, 2014, 136(42), 15086

[60] Apple E F. Investigations in the $CuGaS_2$–ZnS and $AgGaS_2$–ZnS systems. J Electrochem Soc, 1958, 105(5), 251

[61] Liu Z Y, Tang A W, Wang M, et al. Heating-up synthesis of cadmium-free and color-tunable quaternary and five-component Cu−In−Zn−S-based semiconductor nanocrystals. J Mater Chem C, 2015, 3(39), 10114

[62] Zeng B, Chen F, Liu Z, et al. Seeded-mediated growth of ternary Ag−In−S and quaternary Ag−In−Zn−S nanocrystals from binary Ag_2S seeds and the composition-tunable optical properties. J Mater Chem C, 2019, 7(5), 1307

[63] Chen F, Guan Z Y, Tang A W. Nanostructure and device architecture engineering for high-performance quantum-dot light-emitting diodes. J Mater Chem C, 2018, 6(41), 10958

[64] Liu Z M, Liu J, Huang Y B, et al. From one-dimensional to two-dimensional wurtzite $CuGaS_2$ nanocrystals: non-injection synthesis and photocatalytic evolution. Nanoscale, 2019, 11(1), 158

[65] Cheng Y, Wang Y S, Bao F, et al. Shape control of monodisperse CdS nanocrystals: Hexagon and pyramid. J Phys Chem B, 2006, 110(19), 9448

[66] Liu Z M, Tang A W, Liu J, et al. Non-injection synthesis of L-shaped wurtzite Cu−Ga−Zn−S alloyed nanorods and their advantageous application in photocatalytic hydrogen evolution. J Mater Chem A, 2018, 6(38), 18649

[67] Xu Y, Xu R. Nickel-based cocatalysts for photocatalytic hydrogen production. Appl Surf Sci, 2015, 351(1), 779

[68] Alivisatos A P. Semiconductor clusters, nanocrystals, and quantum dots. Science, 1996, 271(5251), 933

[69] Huang E W, Yao X L, Wang W C, et al. SnS_2 nanoplates with specific facets exposed for enhanced visible-light-driven photocatalysis. ChemPhotoChem, 2016, 1, 1

[70] Liu M, Piao L, Zhao L, et al. Anatase TiO_2 single crystals with exposed {001} and {110} facets: facile synthesis and enhanced photocatalysis. Chem Commun, 2010, 46, 1664

[71] Zhou P, Yu J G, Jaroniec M. All-solid-state Z-scheme photocatalytic systems. Adv Mater, 2014, 26(29), 4920

[72] Cunningham P D, Boercker J E, Foos E E, et al. Enhanced multiple exciton generation in quasi-one-dimensional semiconductors. Nano Lett, 2011, 11(8), 3476

[73] Yang Y J, Tang D M, Zhang C, et al. "Protrusions" or "holes" in graphene: which is the better choice for sodium ion storage. Energy Environ Sci, 2017, 10(4), 979

[74] Huynh W U, Dittmer J J, Alivisatos A P. Hybrid nanorod-polymer solar cells. Science, 2002, 295, 2425